NRL Report 6623

Some Basic Aspects of Radar Target Imaging

HENRY A. BROWN

Tracking Branch
Radar Division

November 15, 1967

APPROVED FOR PUBLIC
RELEASE - DISTRIBUTION
UNLIMITED

NAVAL RESEARCH LABORATORY
Washington, D.C.

CONTENTS

Abstract	ii
Problem Status	ii
Authorization	ii
INTRODUCTION	1
FOURIER INTEGRAL REPRESENTATION OF IMAGING	2
POINT SOURCE TARGETS	3
RESOLUTION REQUIREMENTS	7
SAMPLING OF THE FAR FIELD	10
IMAGING INTEGRAL EVALUATION BY LINEAR INTERPOLATION	12
IMAGING INTEGRAL EVALUATION BY FILON'S METHOD	15
IMAGE PEAK POSITION ERROR	19
PLUS-MINUS PHASE APPROXIMATIONS	21
THE CONSTANT-RANGE AND PLANAR APERTURE DIFFERENCE	21
SUMMARY	22
ACKNOWLEDGMENTS	23

ABSTRACT

The classical basis of resolution as applied to radar target imaging has been investigated with reference to point source targets in one dimension and their associated images. The imaging process can be represented by a Fourier integral operation on modified planar aperture data; two methods of evaluating this integral by a digital computer are linear interpolation and Filon's method. Curves were prepared which illustrate the aperture-resolution relationship and the sampling element placement within the aperture. Image distortion due to finite aperture size and to approximations of the far-field phase were examined by generating point source images on a computer and found to be distorted both in peak position and amplitude for finite apertures. Although phase correction for the distance between the constant-range surface and the planar aperture was shown by example to be essential for imaging, useful images can be obtained by such crude approximations as making plus or minus phase assignments to alternate lobes of the far-field pattern.

PROBLEM STATUS

This is an interim report; work on the problem is continuing.

AUTHORIZATION

NRL Problem R02-14
Project RF-001-02-41-4005

Manuscript submitted July 31, 1967.

SOME BASIC ASPECTS OF RADAR TARGET IMAGING

INTRODUCTION

The problems associated with radar target imaging are quite fundamental and should be clearly understood before any attempt to circumvent the obstacles is undertaken. The purpose of this report is to describe the basic imaging problem and to establish quantitative measures of imaging capability in the microwave region. To concentrate on the essential principles we will describe the imaging problem in one dimension for no relative motion between the target and the data collecting aperture. Once the fundamental relationships are established, generalization into two dimensions is only a matter of mathematical manipulation.

After the appropriate coordinate transformations are performed to account for the geometry of the situation, the basic problem can be well described by the Fourier integral. Two methods of evaluating this integral are shown in this report for sampled data input.

Electromagnetic field theory gives a relation between the target current and the far field. By the proper manipulation the inverse of this relation yields the target current as a function of the measured far field. For targets extending many wavelengths the current intensity roughly corresponds to the shape of the target, so identification is essentially visual after smoothing of the current variations; this is the case of object identification with coherent light. For targets extending only several wavelengths or less the correspondence between the current and the geometrical shape of the object is less apparent than for larger targets, and this lack of correspondence will be illustrated in the target images studied.

The principles studied in this report apply to conventional holographic techniques as well as to imaging with antenna arrays. Formation of a hologram on a photographic plate is merely a convenient analog method of two-dimensional heterodyning of spatial frequencies. If the same input information were available to a digital computer, the identical, if not better, image could be reproduced in time, because the same imaging principles herein discussed apply. Of course the big "if" here is the matter of input information form. It would be exceedingly difficult, for example, to measure experimentally the phase and amplitude of the far field from a small model at light frequencies.

Imaging with microwave arrays has generally taken the form of obtaining from the coherently processed output of all elements a single output which produces a high-gain, narrow-beamwidth antenna pattern. The price for this method is high sidelobes for the narrow beamwidth and the necessity of scanning the beam either electronically or mechanically over the target region of interest. An improvement in antenna gain is usually obtainable by this scanning.

The experimental method described herein of obtaining the far-field data incorporates no special beamforming, tapering, or supergain technique, thereby permitting concentration on the fundamentals involved. Phase and amplitude information is separately available from each array element, so the end result of the processing is an image without beam scanning. The disadvantage is the reduction in antenna gain from the array factor to the sampling element pattern factor. Since this is not a system proposal, the gain-reduction is justified on pedagogical grounds. To illustrate the basic concepts of

resolution and diffraction limited imaging as clearly as possible targets will be considered which are isotropic point sources, and the terms "targets" and "sources" will be used interchangeably.

FOURIER INTEGRAL REPRESENTATION OF IMAGING

Consider a one-dimensional target with a current distribution $I(x)$ in plane P_T which lies parallel to an aperture plane P_A, as shown in Fig. 1. If the aperture plane is in the far field of the target, the amplitude of the electric field in the ϕ direction E_ϕ at point y in the aperture plane is related to the current in the target plane by*

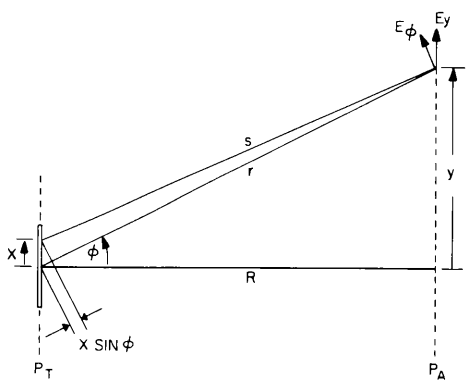

Fig. 1 - The geometry of the target and aperture planes, P_T and P_A

$$dE_\phi(y) = \frac{j60\pi[I]\cos\phi}{s\lambda}\,dx\,, \tag{1}$$

where $[I]$ is the retarded target current as seen at point y in the aperture plane, λ is the wavelength, and ϕ and s are the angle and distance shown in Fig. 1. More specifically, this retarded current is given by

$$[I] = I(x)\,e^{-j\beta s}\,, \tag{2}$$

where $\beta = 2\pi/\lambda$.

If the range R is much greater than the target extent, as is assumed by requiring the aperture plane to be in the target far field, the distance s between target element dx and aperture point y is approximately

$$s \approx \sqrt{R^2 + y^2} - x\sin\phi\,. \tag{3}$$

Under the above assumption the amplitude variation of E_ϕ with x may be neglected so that $s \approx r$ in the denominator of Eq. (1). However, since $\beta x \sin\phi$ may be a significant phase variation with x, the same simplification cannot be made in the retarded current exponential of Eq. (2). Thus far the far field expression of Eq. (1) has reduced to

$$E_\phi = \frac{j60\pi R}{\lambda(R^2+y^2)}\,e^{-j\beta\sqrt{R^2+y^2}}\int_{P_T} I(x)\,e^{j\beta x\sin\phi}\,dx\,. \tag{4}$$

Of interest is the component of E_ϕ in the P_A plane, which is simply

$$\begin{aligned} E_y &= \cos\phi\,E_\phi \\ &= \frac{j60\pi R^2}{\lambda(R^2+y^2)^{3/2}}\,e^{-j\beta\sqrt{R^2+y^2}}\int_{P_T} I(x)\,e^{j\beta x\sin\phi}\,dx\,. \end{aligned} \tag{5}$$

For purposes of manipulation, the following substitutions are made:

$$u = \sin\phi\,, \tag{6a}$$

*J. D. Kraus, "Antennas," New York:McGraw-Hill, 1950, p. 140.

$$v = x/\lambda , \tag{6b}$$

$$G(y) = \text{the integral multiplicative times } \lambda , \tag{6c}$$

and

$$E(u) = E_y/G(y) . \tag{6d}$$

Then Eq. (5) can be written as

$$E(u) = \int_{P_T} I(v)\, e^{j2\pi vu}\, dv , \tag{7}$$

which is the proper form of the Fourier integral having the inverse

$$I(v) = \int_{P_A} E(u)\, e^{-j2\pi vu}\, du . \tag{8}$$

Therefore, since the Fourier transform Eq. (7) possesses the inverse Eq. (8), the target current $I(x)$ can be expressed explicitly as a function of the aperture field as follows:

$$I(x) = \frac{\lambda}{j60\pi} \int_{P_A} E_y(y)\, e^{j\beta\left(\sqrt{R^2+y^2} - \frac{xy}{\sqrt{R^2+y^2}}\right)}\, dy . \tag{9}$$

The physical significance of the exponential term in Eq. (9) will be discussed later in relation to two point sources.

The integral of Eq. (9) can be put into the Fourier integral form of Eq. (8) simply by letting

$$E[u(y)] = \frac{R\lambda\, e^{j\beta\sqrt{R^2+y^2}}}{j60\pi \cos^2\phi} E_y(y) , \tag{10}$$

and the integral form of Eq. (8) will be termed the imaging integral. In other words, the target current (the image) $I(x)$ can be found from the far-field phase and amplitude in the aperture plane P_A by the Fourier transformation if the multiplicative factor in Eq. (10) is applied before the transformation is taken. Note also that the transformation variable is $u = \sin\phi$, which is nonlinear with the aperture variable y except for small values of y compared with range. However, as will be shown later, resolution requirements at microwave frequencies demand that the aperture extent be comparable with the target range, so that the u variable must be retained in the Fourier transformation.

It should also be observed that in the Fourier transform pair as expressed in Eqs. (7) and (8), if the target extent in plane P_T is finite, the aperture extent in plane P_A must be infinite for Eq. (8) to yield exactly the target current $I(v)$. In any physical case the aperture is finite in extent, so the inverse Eq. (8) does not yield an exact replica of the current but rather what is termed a diffraction-limited image of the target. The effect on the target image of a finite aperture is discussed further under resolution requirements.

POINT SOURCE TARGETS

For a basic study of radar target imaging it is convenient and instructive to work with isotropic point sources, since the far field from these sources can be easily formulated and the imaging integral readily evaluated. As the first example consider two

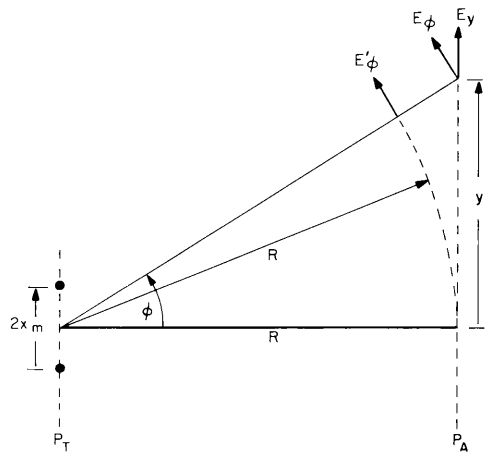

Fig. 2 - Two isotropic point sources in the target plane P_T in relation to the constant-range far-field E'_ϕ and the aperture plane P_A

isotropic point sources of equal amplitude and phase, as shown in Fig. 2. The far field E'_ϕ from this target at a constant range R by Eq. (1) is simply

$$E'_\phi = \frac{j60\pi}{R\lambda} \int_{P_T} \delta(x \pm x_m)\, e^{-j\beta(R \pm x_m \sin\phi)}\, dx$$

$$= \frac{j120\pi}{R\lambda}\, e^{-j\beta R} \cos(\beta x_m \sin\phi)\ , \tag{11}$$

where $\delta(x)$ is the Dirac delta function. The $\cos\phi$ amplitude factor does not appear because the points are isotropic.

The field in the aperture plane is related to the field along the constant range surface by

$$E_y = \cos\phi\, E_\phi$$

$$= \frac{R^2}{R^2 + y^2}\, e^{-j\beta\left(\sqrt{R^2+y^2} - R\right)} E'_\phi\ . \tag{12}$$

In Eq. (12) the $\cos\phi$ term simply expresses the difference in linear polarization between E_ϕ and E_y, and the remainder of the multiplicative factor expresses the attenuation and phase lag introduced by the path length difference between the constant range surface and the aperture plane.

Substitution of Eq. (11) into Eq. (12) gives

$$E_y = \frac{j120\pi}{\lambda} \frac{R}{R^2 + y^2}\, e^{-j\beta\sqrt{R^2+y^2}} \cos\left(\beta x_m \frac{y}{\sqrt{R^2 + y^2}}\right). \tag{13}$$

Comparison of this expression for the far field in the aperture plane from two point sources with the general expression for the imaging integral of Eq. (9) reveals a physical significance for the exponential terms in the imaging integral. The $\beta\sqrt{R^2 + y^2}$ term is a geometrical phase factor arising from the planar shape rather than a spherical (or circular) arc shape of the aperture plane. In an actual experiment this phase factor term would be $\beta(\sqrt{R^2 + y^2} - R)$ for a phase reference at the aperture center of $y = 0$ rather than at the target center of $x = 0$. The $xy/\sqrt{R^2 + y^2}$ term represents the constructive and destructive interference rings which occur at regular intervals in the $u = \sin\phi$ coordinate on the constant range surface. This interference pattern can be projected radially onto the aperture plane in monotonically increasing intervals with y.

In the subsequent discussion the far-field E'_ϕ along the constant-range surface will be examined rather than the field in the aperture plane and will be called the constant-range E-field. This constant-range field can easily be determined from the experimentally measured field in the aperture plane by multiplication of the constant-range correction factor $F(y)$, which is

$$F(y) = \frac{R^2 + y^2}{R^2}\, e^{j\beta\left(\sqrt{R^2+y^2} - R\right)}. \tag{14}$$

The reciprocal of this factor appears in Eq. (12).

Of course this constant-range E-field could be measured directly by using a circular arc aperture which was centered on the target. In such a case, the $F(y)$ factor could be ignored and the measured data used without correction in the imaging integral of Eq. (8).

The magnitude of the constant-range correction factor is shown in Fig. 3 with the aperture position variable normalized with respect to the target range. As can be seen from this figure the constant-range E-field and the planar aperture E-field magnitudes differ less than 1 db within any aperture whose total extent is less than 70 percent of the range. This means that the magnitude of this correction factor may be of secondary importance in the imaging process.

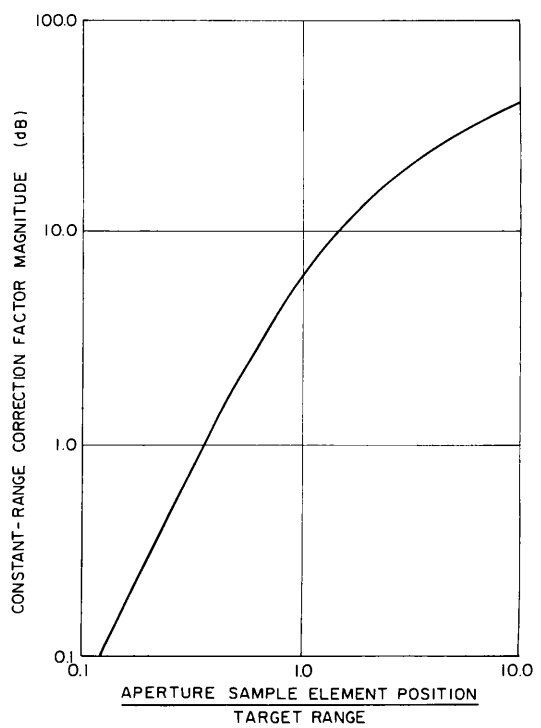

Fig. 3 - The magnitude of the constant-range correction factor $F(y)$ as a function of the position in the aperture of the sample element, normalized with respect to target range

The phase angle of this $F(y)$ correction factor is a different matter entirely, and is shown in Fig. 4. Since this angle depends on both sample element position within the planar aperture and on wavelength, three orders of magnitude of range/wavelength are shown. At X band (λ = 0.1 ft) the curves correspond to ranges of 10, 100, and 1000 ft. Observe that for a total aperture extent of 20 ft and for a range of 100 ft at X band the correction factor angle varies from 0° at the aperture center up to 1800° at the aperture extremity. Quite obviously the phase angle of $F(y)$ must be considered in imaging by Fourier transformation using planar aperture information.

To illustrate the manner of the amplitude and phase variations involved in the constant-range E-field, consider three isotropic point sources of equal amplitude and phase in the target plane with a spacing ratio of 1:d. The constant-range far field is then

$$E'_\phi = \frac{j60\pi}{R\lambda} e^{-j\beta R}\left[1 + e^{j\beta u} + e^{-j\beta du}\right]. \tag{15}$$

The normalized amplitude and the phase referenced to that at $y = 0$ of this constant-range far field is shown in Fig. 5 for three spacing ratios.

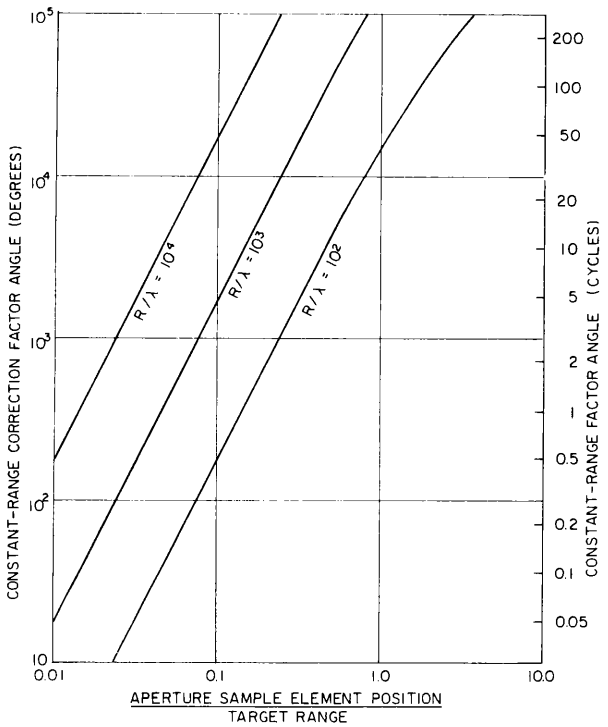

Fig. 4 - The phase of the constant-range correction factor $F(y)$ as a function of the position in the aperture of the sample element, normalized with respect to target range

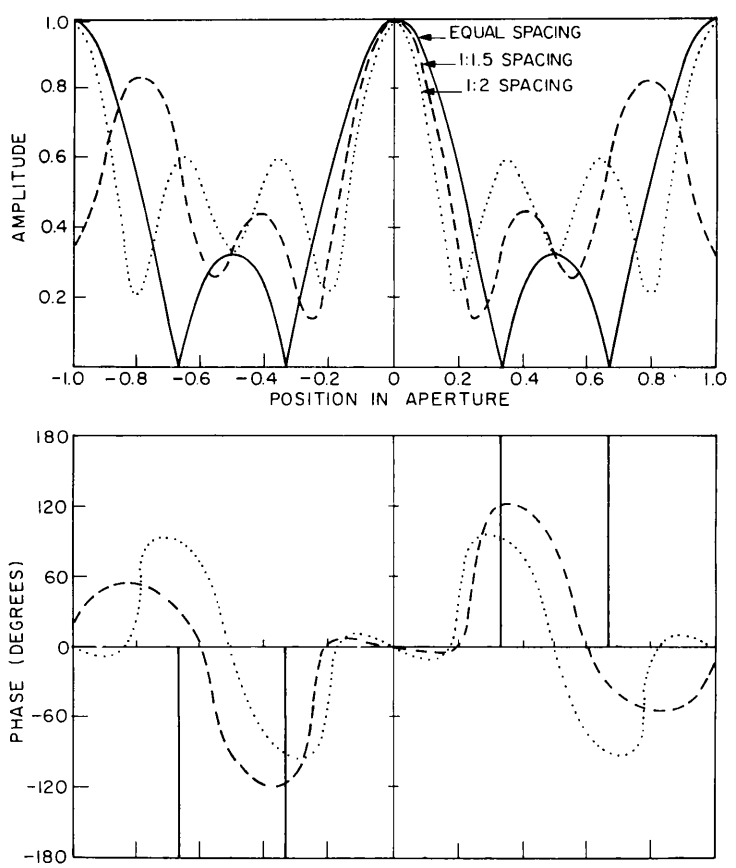

Fig. 5 - The amplitude and phase of the constant-range far field from three isotropic point sources for three spacing ratios

For equal spacing, $d = 1$ and the field is simply

$$E'_\phi = \frac{j60\pi}{R\lambda} e^{-j\beta R}(1 + 2\cos\beta u) , \tag{16}$$

for which the phase (when referenced to the aperture center) is either 0° or 180°. For any unequal spacing the phase across the spherical constant-range surface is continuous but may vary quite rapidly with position u. Only because the point sources are of equal amplitude and phase is the amplitude pattern an even function of position u and the phase an odd function of u. In general this symmetry does not exist for more complex targets.

RESOLUTION REQUIREMENTS

In any physical situation the antenna aperture is necessarily finite in extent, which, when the imaging integral of Eq. (8) or Eq. (9) is applied, results in a diffraction limited image of the target or object. If the aperture is large enough, the resulting image will be a recognizable replica of the original object. One quantitative measure of "large enough" is derived from the concept of resolution.

Consider again the two isotropic point sources of Fig. 2 which produce a constant-range far field of the form

$$E'_\phi = K\cos(\beta x_m \sin\phi) , \tag{17}$$

where $2x_m$ is the separation of the two points. It is evident that this far field is simply a cosinusoidal variation along the constant-range surface in the $u = \sin\phi$ coordinate. Hence the image is simply the Fourier transform of a finite segment of a cosine pattern, the length of which is determined by the finite aperture extent. More specifically, the image will be

$$\begin{aligned} I(x) &= K\int_{-U}^{U} e^{-j\beta xu}\cos\beta x_m u\,du \\ &= 2KU\frac{\sin\beta U(x \pm x_m)}{\beta U(x \pm x_m)} , \end{aligned} \tag{18}$$

where the aperture extent along the constant-range surface is $2U$. The diffraction limited image of two points is then the sum of two sinc functions located at $x = \pm x_m$. (A sinc function is defined as $\operatorname{sinc} x = (\sin\pi x)/\pi x$.)

If the aperture is such that exactly one-half cycle of the cosine spatial variation is included within the aperture, i.e., $U = \lambda/4x_m$, the first null of either of the two sinc functions is congruent with the maximum of the other sinc function; this is termed Rayleigh resolution. In the resultant image, as shown in Fig. 6 (left), the two points are not quite resolved.

If, on the other hand, exactly one full cycle of the cosine spatial variation is included within the aperture, i.e., $U = \lambda/2x_m$, the first null of either of the two sinc functions is congruent with the first null of the other sinc function, and the two points are well resolved, as shown in Fig. 6 (right). This case will be termed null resolution because of the congruency of the nulls and will serve as a useful definition for resolution in this report.

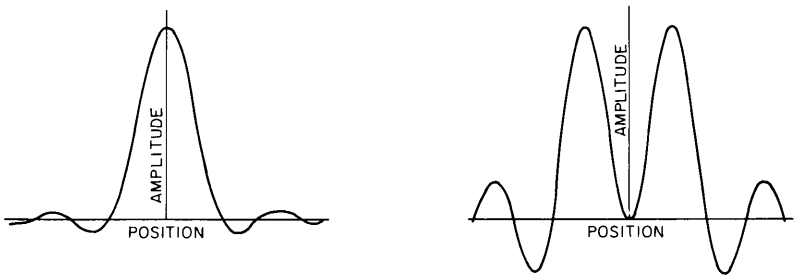

Fig. 6 - The image amplitude of two equal coherent isotropic point sources separated (left) by one Rayleigh resolution cell and (right) by one null resolution cell

The utility of the Rayleigh resolution criterion is found not in the coherent illumination case, to which this investigation is restricted, but in the incoherent illumination case. For two isotropic incoherent sources separated by one Rayleigh resolution cell the intensity of the image is the sum of the squares of the two sinc functions, as shown at the left in Fig. 7. The resultant intensity pattern has a saddle point at the center, thereby resolving the two points. For the coherent case the intensity is the square of the sum of the two sinc functions, i.e., simply the square of the total amplitude as shown at the right in Fig. 7. This image does not have a saddle point at the center, so the separation of the two points is not clearly defined.

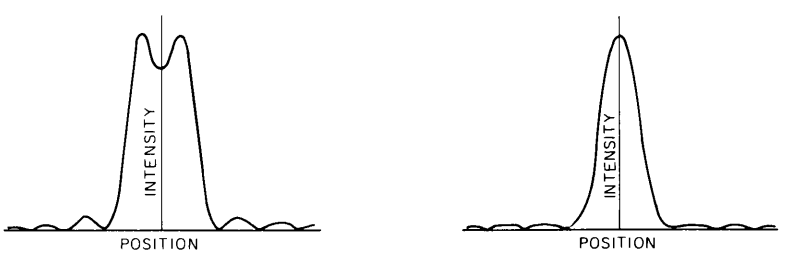

Fig. 7 - The image intensity of two equal isotropic point sources separated by one Rayleigh resolution cell for (left) the incoherent case and (right) the coherent case

These concepts of resolution using the constant-range surface can easily be transferred into requirements on the planar aperture through the $u = \sin \phi$ coordinate. Since for Rayleigh resolution only one-half cycle of the cosine pattern need be included within the aperture, then $\beta x_m \cdot 2U = \pi$ or

$$\beta x_m \frac{y_{\max}}{\sqrt{R^2 + y_{\max}^2}} = \frac{\pi}{2} , \tag{19}$$

which can be solved for the aperture required for Rayleigh resolution as

$$A_{\text{Rayleigh}} = 2y_{\max} = \frac{2\lambda R}{\sqrt{16x_m^2 - \lambda^2}} . \tag{20}$$

It is convenient to define the separation of the two points for this resolution limit as the resolution cell $r' = 2x_m$, which gives

$$A_{\text{Rayleigh}} = \frac{2\lambda R}{\sqrt{4r'^2 - \lambda^2}} \tag{21}$$

According to Eq. (21) this Rayleigh resolution cell cannot be smaller than a half wavelength, which indeed was the basis of Rayleigh resolution in the first place, as discussed above in relation to the Fourier transformation.

For null resolution one full cycle of the cosine pattern needs to be included within the aperture. Hence $\beta x_m U = \pi$ or

$$A_{\text{null}} = 2y_{\max} = \frac{2\lambda R}{\sqrt{r'^2 - \lambda^2}} \,. \tag{22}$$

Again the definition of resolution appears in that the resolution cell r cannot be less than one wavelength.

By normalizing the aperture with respect to range and the resolution cell r' with respect to wavelength the aperture-resolution relationship can be shown in the useful form of Fig. 8 for both the Rayleigh and null resolution criterions. Note that if the

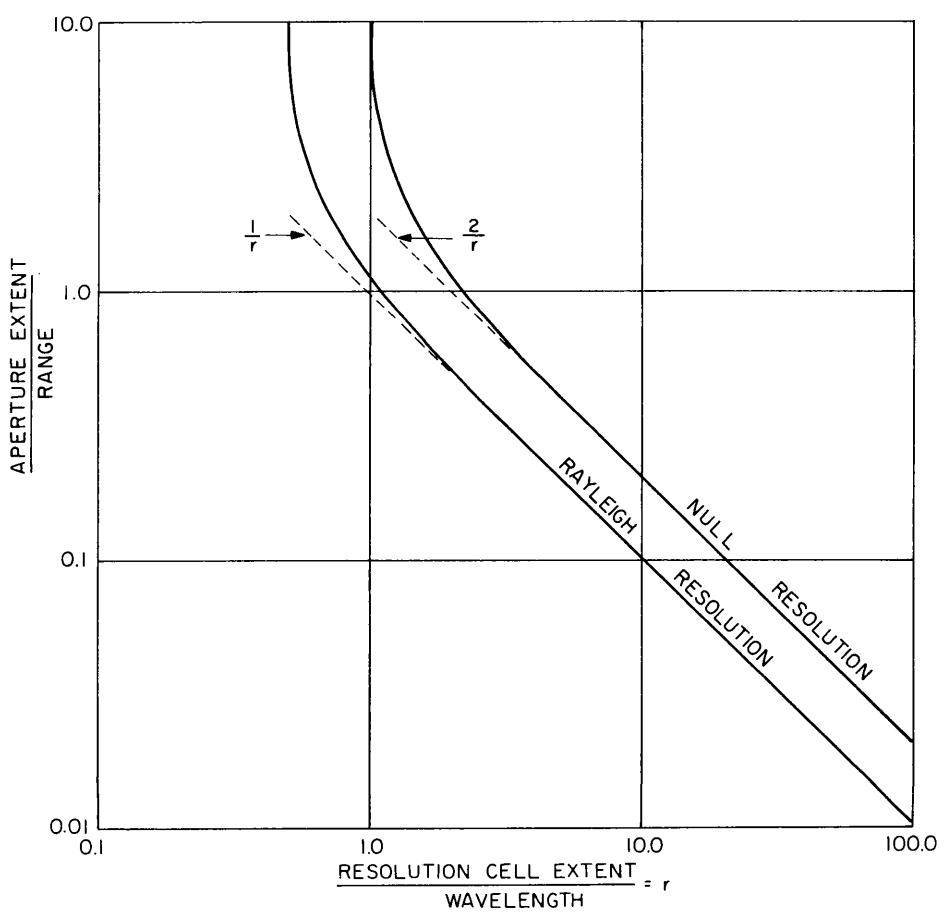

Fig. 8 - The aperture extent, normalized with respect to target range, vs resolution cell extent, normalized with respect to wavelength, for the null and Rayleigh resolution criterion

resolution cell is greater than about four wavelengths, the required aperture for null resolution is given approximately by $2/r$. For Rayleigh resolution and a resolution cell greater than two wavelengths the required aperture is approximately $1/r$. For example, at X band and a target range of 100 ft a null resolution cell of 1 ft would require a 20-ft aperture and a Rayleigh resolution cell of 1 ft would require a 10-ft aperture.

SAMPLING OF THE FAR FIELD

One method of obtaining the far field in the aperture plane is by an odd number of sampling antennas rigidly fixed along a stable support. Phase can be referenced to the center element, as can amplitude measurements, or to any other nonzero amplitude position. The odd number of elements can conveniently provide the center element as the zero positional reference. In applying the imaging integral of Eq. (8) it is expedient to have the samples equally spaced in the $u = \sin\phi$ coordinate which, when projected onto the aperture plane, gives an increasing element separation out from the center of the array. Letting N equal the odd number of sampling elements, the constant spacing in the u coordinate for null resolution is

$$\Delta u_{\text{null}} = \frac{2}{r(N-1)} . \tag{23}$$

The ith sampling element in the aperture plane, counting from the center outward, is located at

$$\frac{y_i}{R} = \frac{i\Delta u}{\sqrt{1-(i\Delta u)^2}} , \qquad i = 0, 1, 2, \ldots, \frac{N-1}{2} . \tag{24}$$

This equation as a function of the product of the element counter i and the constant spacing Δu of the u coordinate is shown in Fig. 9. Notice that the spacing is approximately constant as long as the product of i and Δu is less than 0.2. This implies that if the null resolution cell is greater than five wavelengths, the sampling elements may be equally spaced in the aperture plane.

The position of these sample elements in the aperture plane may also be expressed less generally by fixing the number of sample points and by letting the element counter divided by the resolution cell extent i/r be the independent variable; the expression then is

$$\left(\frac{y_i}{R}\right)_{\text{null}} = \frac{i/r}{\sqrt{\left(\frac{N-1}{2}\right)^2 - \left(\frac{i}{r}\right)^2}} . \tag{25}$$

This relation is shown in Figs. 10 and 11 for several sets of sampling points. Note that sample element taper is significant only out toward the ends of the array and, of course, is symmetrical about the center. For example, for 37 sample points the spacing is constant up to $i/r = 4$ (see Fig. 10), which means that the resolution cell should be greater than 4.5 wavelengths or about 5 wavelengths as stated above from Fig. 9.

The resolution capability of an aperture is determined by the total length of that aperture. In other words, the longest spatial period of the constant-range E-field which will fit into an aperture determines the resolution.

If a target is composed of several equally spaced point sources, the spacing of these sources determines the lowest spatial frequency in the far field. At the other end of the scale the extent of such a target determines the highest spatial frequency in the far field

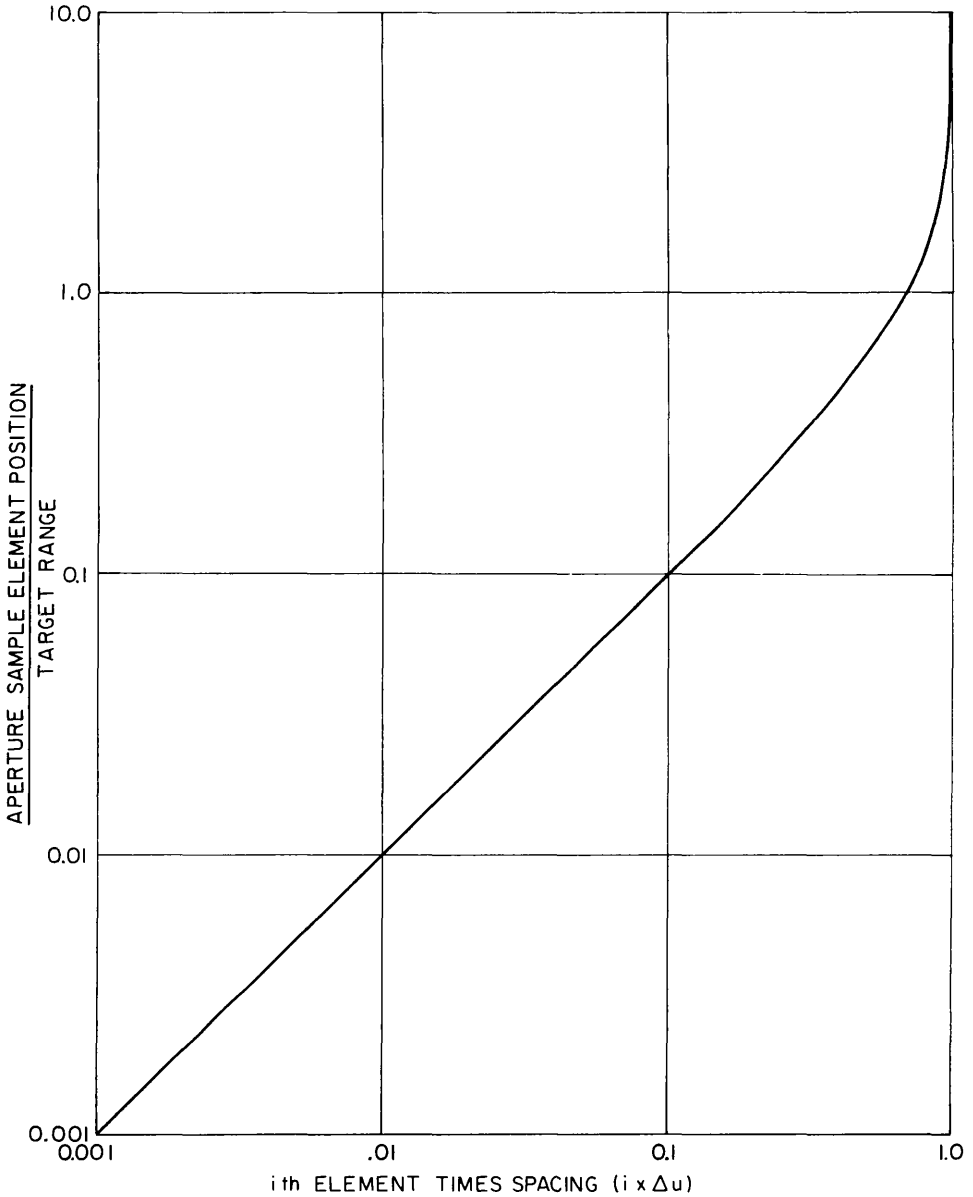

Fig. 9 - The sampling element position within the aperture, normalized with respect to target range, vs the ith sampling element times spacing, where $i = 0, 1, 2, \ldots$ and $\mu = \sin \phi$

and thereby establishes a lower limit on the sample element spacing. This maximum spatial frequency for a target composed of these equally spaced points is $L/2\lambda R$ cycles per meter in the aperture plane, where L is the target extent.

For a target composed of any unequally spaced points the situation is much more complicated. For instance, observe the complex field from three such point sources as shown in Fig. 5. Where for equal spacing the field consists of an average component of relative magnitude 1 and a cosinusoidal spatial component of magnitude 2, for the particular unequal spacings shown an additional spatial harmonic appears. The spatial frequency components coresponding to the three spacings in Fig. 5 are shown in Fig. 12.

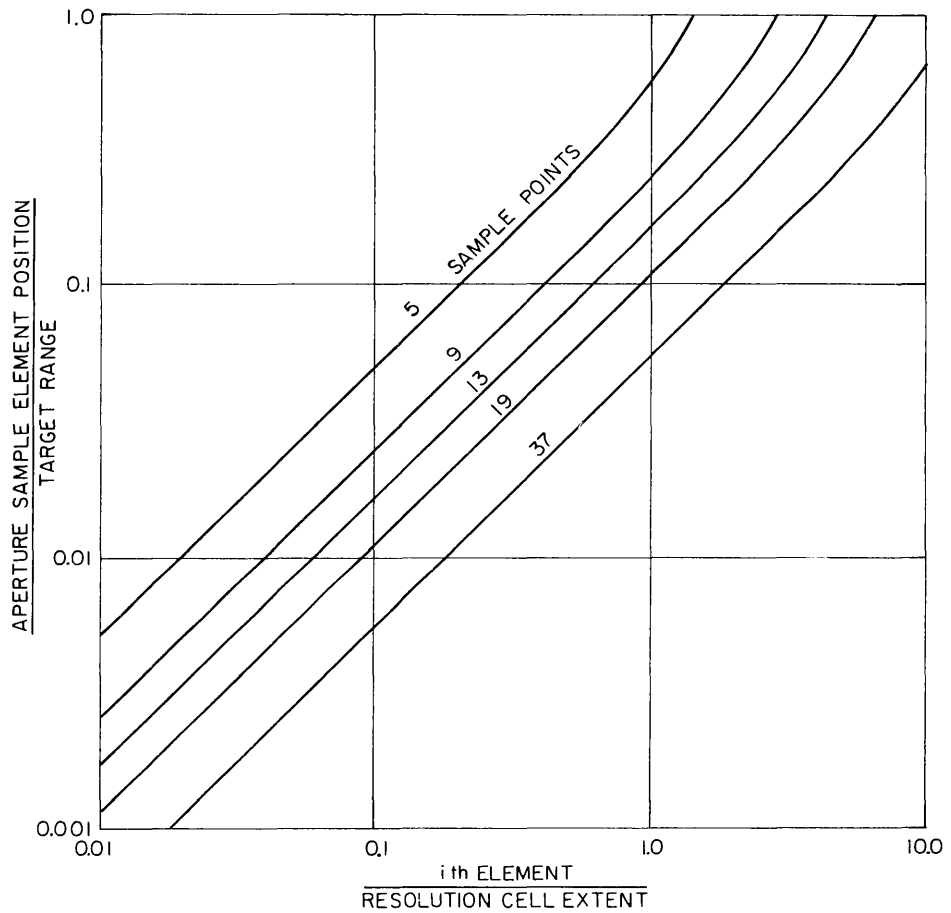

Fig. 10 - The sampling element position within the aperture, normalized with respect to target range, vs the ith sampling element, normalized with respect to the null resolution cell extent, for five sets of total sample points

Only because the point sources are located at integer multiples of the Rayleigh resolution cell does a finite number of spatial frequencies appear in the constant-range far field. For instance, if the spacing ratio were 1:1.4, spatial frequencies at all integer multiples of the fundamental (2π/aperture extent) would exist, as can be shown from Eq. (15). Hence, it is difficult to derive a relation for the maximum spatial frequency (and thereby the sampling rate) in the constant-range far field of a general target beyond that stated above of $L/2\lambda R$ for a line of equally spaced point sources.

IMAGING INTEGRAL EVALUATION BY LINEAR INTERPOLATION

If the imaging process operates on the constant-range far field of a target which has been sampled at a finite number of points, it is necessary to adapt the imaging integral of Eq. (8) to operate on such input data. As previously discussed, range, aperture extent, and wavelength all influence the resolution obtainable and appear in the expression for the image. Since all these parameters are accounted for in the $F(y)$ factor of Eq. (14), the entire imaging integral can be scaled such that only the number of sample points N needs to be considered along with the phase and amplitude of the constant-range far field.

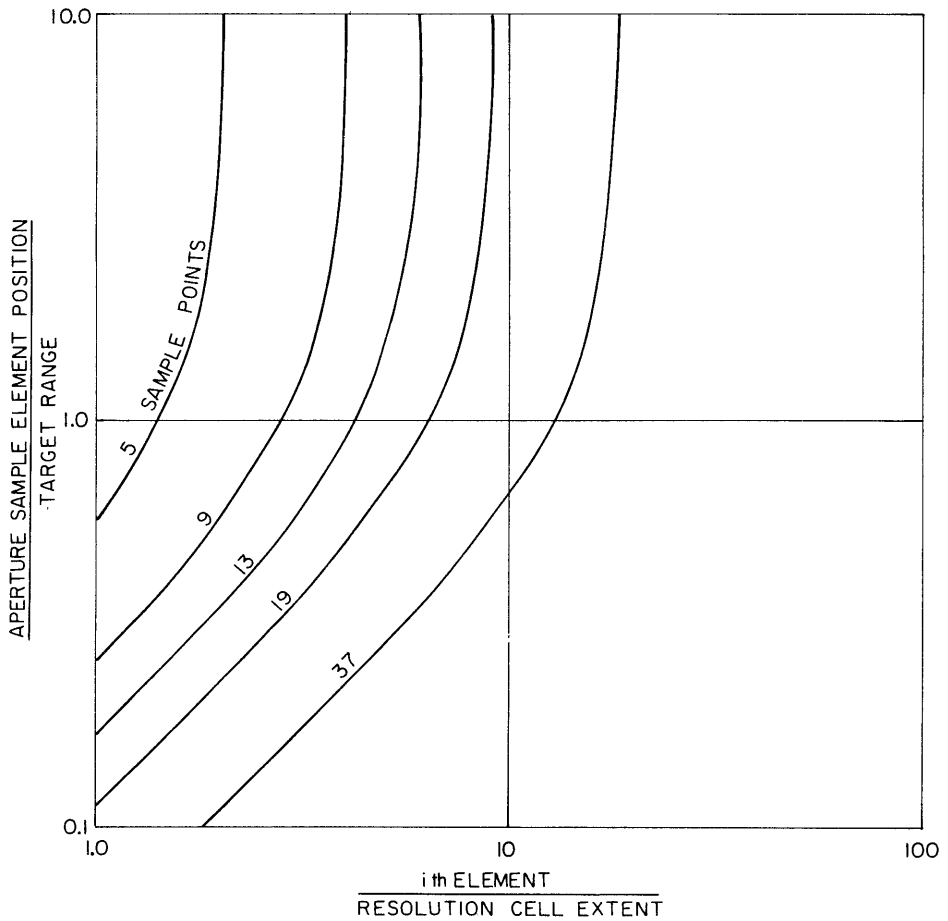

Fig. 11 - The sampling element position within the aperture, normalized with respect to target range, vs the i th sampling element, normalized with respect to the null resolution cell extent, for five sets of total sample points

This scaling is easily accomplished by the substitutions

$$\eta = \frac{N-1}{2U} u , \tag{26a}$$

$$\zeta = 2Uv , \tag{26b}$$

where $2U$ is the total aperture extent in the u coordinate. When Eq. (26) is used and a multiplicative constant is dropped, the imaging integral of Eq. (8) reduces to

$$I'(\zeta) = \frac{1}{N-1} \int_{-\frac{N-1}{2}}^{\frac{N-1}{2}} E(\eta) e^{-j \frac{2\pi}{N-1} \zeta \eta} d\eta . \tag{27}$$

The integrator η now assumes the form of the integer element counter i as used in the discussion of sample element position. For example, for 37 sample points η takes on all the integer values between ± 18, inclusive, and the fundamental spatial frequency is 1/36.

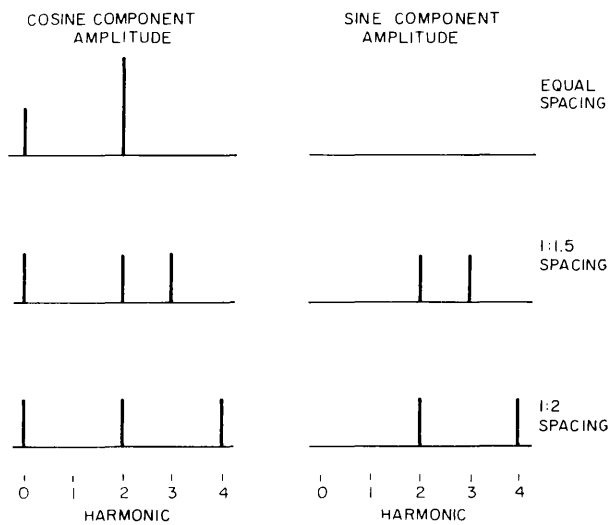

Fig. 12 - The Fourier components of the constant-range far field from three isotropic point sources for three different spacing ratios. The fundamental frequency is $2\pi/(\text{aperture extent})$.

The image plane variable ζ is also conveniently scaled by Eq. (26), since one null resolution cell equals unity in this coordinate regardless of the actual aperture, range, or wavelength.

The imaging integral of Eq. (27) can be further reduced to a finite summation, if some assumption is made as to the variation of $E(\eta)$ between sample points. Suppose that the field can be represented by linear interpolation between sample points in amplitude and in phase. This makes the integrand $E(\eta)$ in the imaging integral a piecewise linear function between the integers in the range $\pm(N-1)/2$. As a result of taking the kth segment of $E(\eta)$, the center of which is located at $\eta = k + (1/2)$, and using the shift theorem of Fourier transforms, the image produced only by this segment is

$$e^{-j\frac{2\pi}{N-1}(k+\frac{1}{2})} \int_{-\frac{1}{2}}^{\frac{1}{2}} E_k\left(\eta - k + \frac{1}{2}\right) e^{-j\frac{2\pi}{N-1}\zeta\eta}\, d\eta . \tag{28}$$

Since superposition is applicable here, the imaging integral of Eq. (27) may be evaluated by summing the products of the Fourier transform of each of the linear segments, the centers of which are shifted to the origin by the shift factor

$$e^{-j\frac{2\pi}{N-1}(k+\frac{1}{2})} \tag{29}$$

By some laborious manipulations the imaging integral can be put in the form

$$I'(\zeta)_{\sigma_k \neq 0} = \sum_{k=-\frac{N-1}{2}}^{\frac{N-1}{2}-1} e^{-j\left[\frac{2\pi}{N-1}(k+\frac{1}{2})\zeta - b_k\right]} \left[B_k \frac{\sin \sigma_k/2}{\sigma_k/2} + \frac{j}{2}\frac{M_k}{\sigma_k/2}\left(\frac{\sin \sigma_k/2}{\sigma_k/2} - \cos\frac{\sigma_k}{2}\right)\right] \tag{30a}$$

$$I'(\zeta)_{\sigma_k=0} = \sum_{k=-\frac{N-1}{2}}^{\frac{N-1}{2}-1} e^{-j\left[\frac{2\pi}{N-1}(k+\frac{1}{2})\gamma - b_k\right]} B_k , \tag{30b}$$

where

$$\sigma_k = m_k - \frac{2\pi}{N-1}\zeta , \tag{31}$$

and the slopes and slope intercepts of the kth shifted segment are

$$M_k = |E_{k+1}| - |E_k| , \qquad m_k = \arg E_{k+1} - \arg E_k , \tag{32a}$$

$$B_k = \frac{1}{2}(|E_{k+1}| + |E_k|) , \qquad b_k = \frac{1}{2}(\arg E_{k+1} + \arg E_k) . \tag{32b}$$

Although this form is seemingly more complex than the integral form it is particularly well suited for evaluation by a digital computer.

The accuracy of this linear interpolation method as a function of the number of sample points was checked by computing and uniformly sampling in the u coordinate for 37, 19, 13, and nine points the constant-range far field from two isotropic point sources separated by one null resolution cell. The true diffraction limited image of these two point sources is

$$I'(\zeta) = \frac{\sin \pi(\zeta \pm 1)}{\pi(\zeta \pm 1)} \tag{33}$$

and was compared with the image computed from the linear interpolation formula of Eq. (30). For 13 sample points or more the error was less than 1 percent for $|\zeta| < 7$. Beyond $|\zeta| = 7$ the image is more than 11 db down, and the image is beyond the third sidelobe of the sinc function. Here the percent error loses much of its meaning except as an order of magnitude. For nine sample points the error was less than 6 percent for $|\zeta| < 6$.

This error as a function of the number of sample points depends greatly upon the target. If the constant-range far field from a three-point-source target with a 1:1.5 spacing ratio is nine point sampled as shown in Fig. 13, a fairly erroneous image results as compared with the exact image, as shown in Fig. 14. Even though this sampling rate was sufficient to produce an accurate image for the two-point target, it was not sufficient when an additional source 1.5 null resolution cells away was added. Even though the highest frequency component in the constant-range far field is 3ω and sampling is at 9ω, the distorted image results not from aliasing but from truncation to a finite number of samples. Since the single spatial frequency from two points was well represented by 13 samples, a rule of thumb would be to sample the constant-range far field at least 10 times the highest spatial frequency within the sampling aperture.

IMAGING INTEGRAL EVALUATION BY FILON'S METHOD

Another method of evaluating the imaging integral is to obtain the Fourier coefficients of the constant-range far field which provide linear weighting values for the summation of sinc functions in the image plane. First the sufficiency of the Fourier coefficients for imaging integral evaluation will be shown.

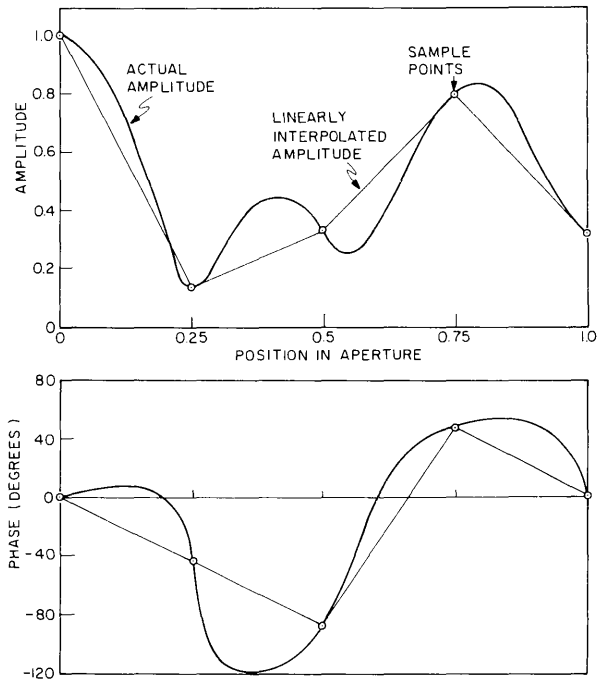

Fig. 13 - One-half of the symmetrical constant-range far field as measured from the aperture center from three isotropic point sources with a 1:1.5 spacing ratio, showing the approximation of linear interpolation between nine sample points

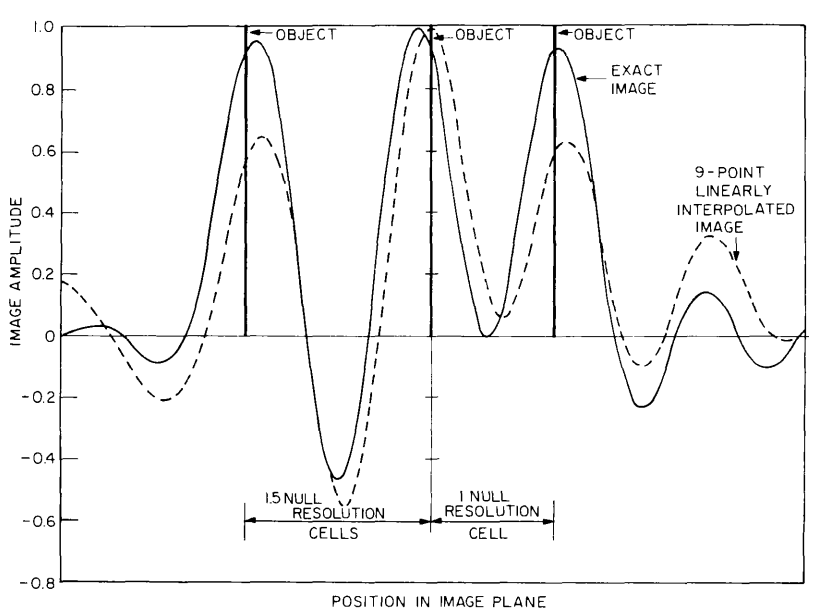

Fig. 14 - The image amplitude of three isotropic point sources resulting from nine-point linear interpolation of the constant-range far field of Fig. 13 along with the true diffraction limited image and the original objects

Since the constant-range far field magnitude and phase are known, it is a simple matter to express the field in complex form as

$$E(\eta) = E_r(\eta) + j\, E_i(\eta) \tag{34}$$

and the real and imaginary components of the field in complex Fourier series form as*

$$E_r(\eta) = \sum_{k=-\infty}^{\infty} c_r\, e^{j\omega k\eta} \tag{35a}$$

$$E_i(\eta) = \sum_{k=-\infty}^{\infty} c_i\, e^{j\omega k\eta} . \tag{35b}$$

These complex Fourier coefficients are obtained from

$$c_r = \frac{\omega}{2\pi} \int_{-\pi/\omega}^{\pi/\omega} E_r(\eta)\, e^{-j\omega k\eta}\, d\eta \tag{36a}$$

$$c_i = \frac{\omega}{2\pi} \int_{-\pi/\omega}^{\pi/\omega} E_i(\eta)\, e^{-j\omega k\eta}\, d\eta \tag{36b}$$

and are related to the more familiar real Fourier coefficients by

$$c_k = \frac{1}{2}\,(a_k - j\,b_k) , \qquad k > 0 ; \tag{37a}$$

$$c_k = \frac{1}{2}\, a_0 , \qquad k = 0 ; \tag{37b}$$

$$c_k = \frac{1}{2}\,(a_k + j\,b_k) , \qquad k < 0 . \tag{37c}$$

Substitution of Eq. (35) into Eq. (34) gives

$$E(\eta) = \sum_{k=-\infty}^{\infty} (c_r + j\,c_i)\, e^{j\omega k\eta} , \tag{38}$$

which when substituted into the imaging integral gives

$$I'(\zeta) = \frac{\omega}{2\pi} \int_{-\pi/\omega}^{\pi/\omega} \sum (c_r + j\,c_i)\, e^{j\omega k\eta}\, e^{-j\omega\zeta\eta}\, d\eta$$

$$= \sum_{k=-\infty}^{\infty} (c_r + j c_i)\, \frac{\sin \pi(k-\zeta)}{\pi(k-\zeta)} , \tag{39}$$

*R. W. Hamming, "Numerical Methods for Scientists and Engineers," New York:McGraw-Hill, p. 302, 1962.

which is simply the summation of sinc functions located at integer positions in the image plane and weighted by the complex Fourier coefficients of the constant-range far field within the finite aperture.

These complex coefficients of the complex field representation of $E(\eta)$ are related to the real Fourier coefficients by

$$c_r + j c_i = \frac{1}{2}\left[a_r + b_i + j(a_i - b_r)\right], \qquad k > 0\,; \tag{40a}$$

$$c_r + j c_i = \frac{1}{2}\left[a_r + j a_i\right], \qquad k = 0\,; \tag{40b}$$

$$c_r + j c_i = \frac{1}{2}\left[a_r - b_i + j(a_i + b_r)\right], \qquad k < 0\,. \tag{40c}$$

The a's are the cosine components of the real (r) and imaginary (i) components of $E(\eta)$, and the b's are the sine components of the corresponding components of $E(\eta)$.

Examination of Eq. (40) reveals that the image is a real valued function if and only if $a_i = b_r = 0$. This is to say that the real part of the field E_r must be an even function of position η and the imaginary part of the field E_i must be an odd function of position relative to the aperture center for the image to be real. If the equations are viewed in polar form, it is seen that the magnitude must be even with position and the phase must be an odd function with position. Furthermore this requires all the points on the planar target to be in phase. Since this cannot be expected to hold in general, capability of imaging in the complex domain must still be maintained.

The real Fourier coefficients a and b may be numerically obtained for the real and imaginary parts of the constant-range far field by Filon's method.* In essence this method assumes quadratic interpolation between sets of three adjacent points and thereupon evaluates for the Fourier coefficients. Since the adaptation of Filon's method to the problem at hand is straightforward but quite lengthy, only the final results will be given. For either the real or imaginary part of the constant-range far field the complex Fourier coefficients are

$$(N-1)c_k = j\alpha(-1)^k\left[E\left(\frac{N-1}{2}\right) - E\left(-\frac{N-1}{2}\right)\right] - \frac{1}{2}\beta(-1)^k\left[E\left(\frac{N-1}{2}\right) + E\left(-\frac{N-1}{2}\right)\right]$$
$$+ \beta\sum_{n=1}^{L_2} E\left(2n - \frac{N+3}{2}\right) e^{-j\frac{k\pi}{L_1}(2n-L_1-2)} + \gamma\sum_{n=1}^{L_1} E\left(2n - \frac{N+1}{2}\right) e^{-j\frac{k\pi}{L_1}(2n-L_1-1)}, \tag{41}$$

where the limits of summations and the coefficients are

$$L_1 = \frac{N-1}{2}, \tag{42a}$$

$$L_2 = \frac{N+1}{2}, \tag{42b}$$

$$\theta = \frac{2\pi k}{N-1}, \tag{42c}$$

*L. N. Filon, "On a Quadrature Formula for Trigometric Integrals," Proc. Royal Soc. Edinburgh, 49:38, 1928-29.

$$\alpha_{\theta \neq 0} = \frac{1}{\theta^3} \left[\theta^2 + \theta \sin \theta \cos \theta - 2 \sin^2 \theta\right] , \tag{42d}$$

$$\alpha_{\theta = 0} = 0 , \tag{42e}$$

$$\beta_{\theta \neq 0} = \frac{2}{\theta^3} \left[\theta(1 + \cos^2 \theta) - 2 \sin \theta \cos \theta\right] , \tag{42f}$$

$$\beta_{\theta = 0} = \frac{2}{3} , \tag{42g}$$

$$\gamma_{\theta \neq 0} = \frac{4}{\theta^3} \left[\sin \theta - \theta \cos \theta\right] , \tag{42h}$$

$$\gamma_{\theta = 0} = \frac{4}{3} . \tag{42i}$$

In the relation for the Fourier coefficients (Eq. (41)) the first summation is over the odd numbered sample points and the other summation is over the even numbered sample points. The α, β, and γ coefficients provide the quadratic weights.

To compare the accuracy of Filon's method with the linear interpolation method of imaging integral evaluation the constant-range far field from two isotropic point sources was sampled at 37, 19, 13, and nine points and the image obtained by Filon's method compared with the true diffraction limited image for the same aperture as was done with the linear interpolation method. For 37 sample points the percent error was less than 0.1 percent, for 19 samples the error was less than 1 percent, and for 13 samples the error was less than 10 percent for $|\zeta| < 7$. However, for the nine-sample-point case, a considerably larger error occurred around two of the zero crossings of the sidelobes, as shown in Fig. 15. This error can be directly ascribed to the Fourier analysis of the far field, since a coefficient of -0.0162 was computed by Filon's method to exist at $\zeta = \pm 3$ and similarly another coefficient of 0.0124 to exist at $\zeta = \pm 5$. The only coefficients that should exist are at $\zeta = \pm 1$, the target source positions. Nevertheless, this percent error is rather unimportant in this particular case because of the very small value of the image around these points.

Also shown in Fig. 15 is the percent error in the two-point-source image that is produced by nine-point linear interpolation. Again the 70 percent error at $\zeta = 6.9$ is unimportant because of the small value of the image at the fifth sidelobe. However, since the error is shifted further away from the region of interest, the linear interpolation method may be slightly more preferable than Filon's method.

IMAGE PEAK POSITION ERROR

It should be observed that the positions of the peaks of the true diffraction limited images do not correspond to the exact positions of the objects which they represent. In Fig. 14 the exact image of the three unequally spaced point sources has two peaks slightly to the right of the true source positions and the third peak slightly to the left of the source it represents. A similar distortion of the peak position occurs for the two-point-source image as seen in Fig. 15, where the image peaks lie outside the sources. This position displacement is due to both the finite length of the sample aperture and to the position of the periodic constant-range field with respect to the aperture center.

As an example of image peak position error consider the constant-range far field from two isotropic point sources, which is a cosinusoidal spatial pattern within the

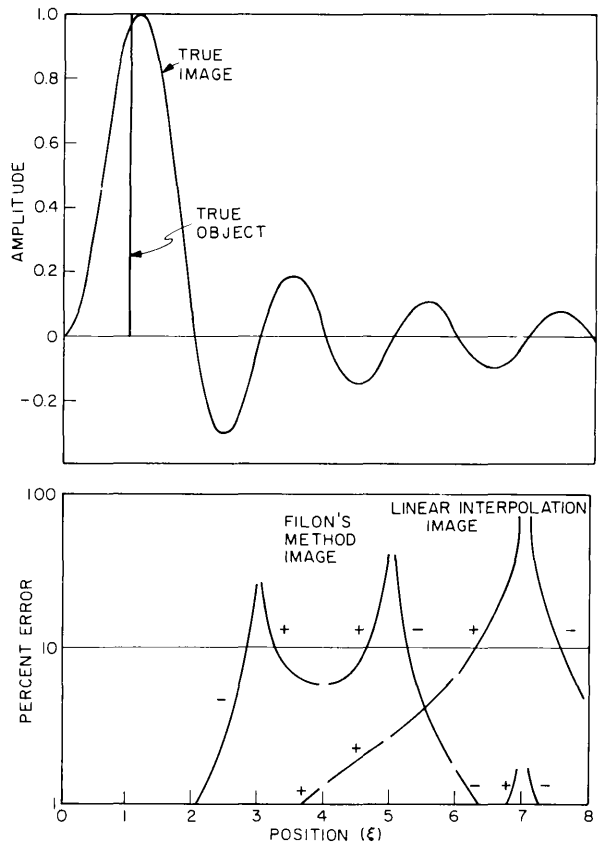

Fig. 15 - One-half of the true diffraction limited image of two isotropic point sources with the percent error in the images of these points as produced by Filon's method and by linear interpolation of the imaging integral, each using nine sample points

aperture. Suppose many sample points are available at a spacing corresponding to 5° of the cosinusoid. This would mean that 37 adjacent sample points would cover exactly one-half cycle of the pattern. When starting with a single half cycle centered in the aperture, observe what happens to the image as two sample points at a time are added onto the ends of the aperture in two ways. When both points are added to the same side, the result is a cosine pattern from $-\pi/2$ to $3\pi/2$ after 36 extra points have been added. The resulting image has its two maxima about 17 percent on the inside of the true object positions. When one sample point is added to each end of the aperture, the result is a cosine pattern from $-\pi$ to π after 36 extra points have been added. The resulting image has its two maxima about 12 percent to the outside of the true object positions. As more of the extra points are added in either of these two ways the positions of the image pattern peaks will oscillate in a decreasing manner about the true object positions, as shown in Fig. 16.

The utility of the null resolution concept in the coherent case again appears in Fig. 16. Note that for ten or less extra sample points divided equally between both sides a -100 percent error occurs. This means that the image has only one peak and that one at zero; i.e., the two point sources are not resolved. The aperture must include more than one-half cycle of the lowest spatial frequency of the constant-range far field in order to resolve the closest pair of points which are producing this spatial frequency in the target.

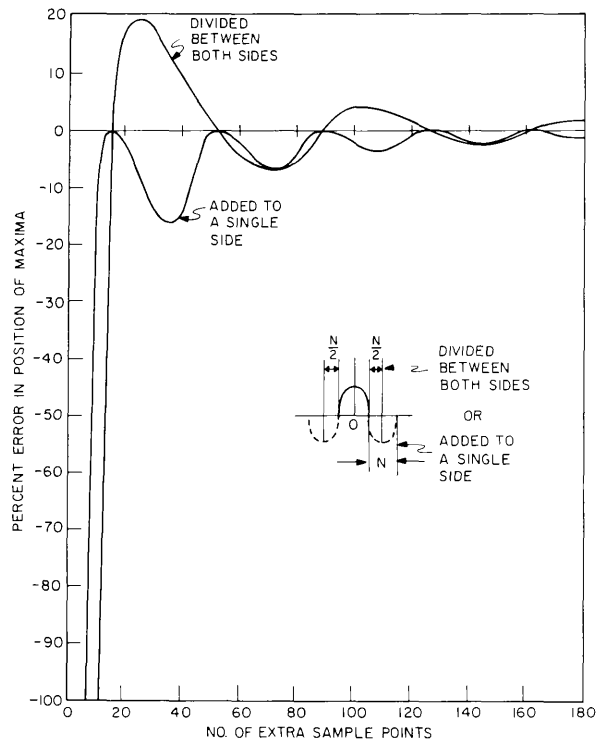

Fig. 16 - The percent error in the image maxima position of two isotropic point sources as a function of the number required for Rayleigh resolution. The spacing between sample points corresponds to 5° of the cosinusoidal constant-range far field.

PLUS-MINUS PHASE APPROXIMATIONS

If it were possible to measure only the magnitude of the constant-range far field and make some approximation to the phase across the aperture, considerable experimental simplification would result. Again, the validity of the approximation depends entirely upon the target under measurement. As an example, take the three-isotropic-point-source target with a 1:1.5 spacing ratio which produces the amplitude and phase far-field patterns shown in Fig. 13. If one has available only the magnitude information, a reasonable approximation to the phase might be to assign a zero phase to the first lobe about the center, a 180° phase to the second lobe, and a zero phase to the third lobe. The result of such an approximation is shown in Fig. 17 along with the true image and actual object. Since the approximated image is symmetrical about the center position, it cannot be determined that the spacing between the point sources is unequal. Otherwise, in a qualitative sense, the phase approximation yields an acceptable image.

THE CONSTANT-RANGE AND PLANAR APERTURE DIFFERENCE

Throughout this discussion the constant-range far field has been used. This field is obtained by applying the $F(y)$ factor of Eq. (14) to the field measured in the planar aperture. This $F(y)$ factor takes into account the reduction in amplitude and the phase delay

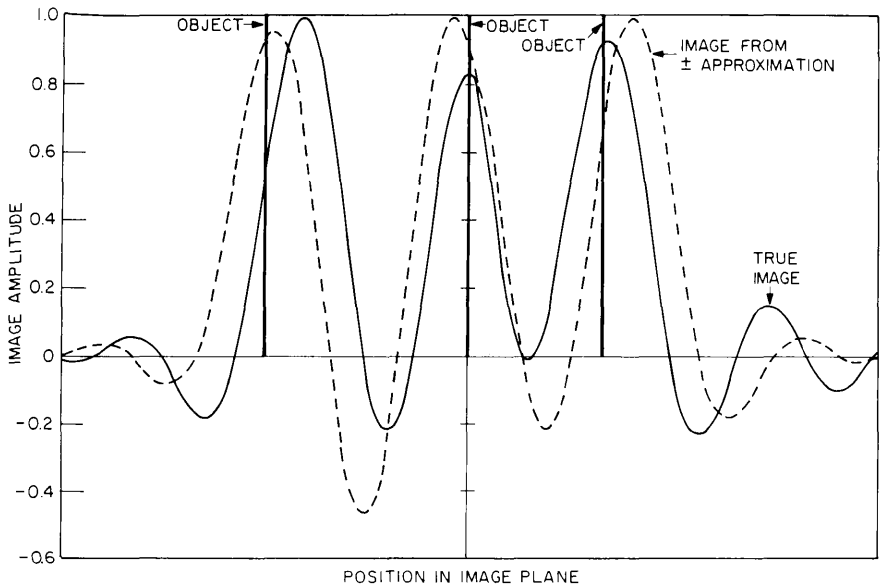

Fig. 17 - The image amplitude of three isotropic point sources resulting from a plus-minus phase approximation of the constant-range far field along with the true diffraction limited image and the original objects

introduced by the distance between the constant-range surface and the planar aperture. Both range and wavelength must be known in order to determine this factor. Since the aperture must be quite large to obtain a reasonable resolution at microwave frequencies, this $F(y)$ factor cannot be neglected.

To illustrate the importance of the $F(y)$ factor, the image of three points with a spacing ratio of 1:1.5 was computed directly by application of the Fourier integral to the planar aperture information without correction with the $F(y)$ factor. The wavelength was 0.1 ft (X band) and the target range was 100 ft. The resulting image was complex and bore no resemblance to the true object or true diffraction limited image, as shown in Fig. 18. No improvement in image quality should be expected if the range were increased unless the aperture extent were also increased to maintain a constant resolution capability.

SUMMARY

The method of examining the radar target imaging problem in this report has been to consider a simple physical situation for obtaining far-field information. The hypothetical experimental arrangement was not chosen to optimize any particular parameter but for an appreciation of the consequences of the classical definition of resolution. These consequences are amply illustrated from the nature of the Fourier integral, which is the imaging operator utilizing far-field amplitude and phase to obtain the target current.

After defining the criterion for resolution on the basis of point source images, the aperture, range, wavelength, and resolution interrelationship can be established. Other factors such as the constant-range and planar-aperture differential distance and the sampling element separation were related to the hypothetical experimental arrangement. The images resulting from unequally spaced point sources were found and related to the demands placed on the experimental measurement technique. Two methods of evaluating the imaging integral by a digital computer were given and compared. It was also noted

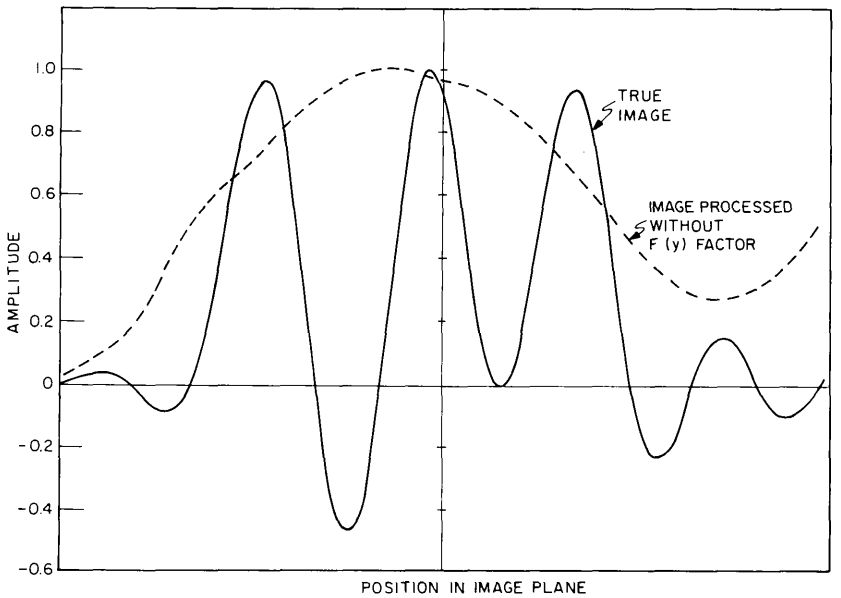

Fig. 18 - The image amplitude of three isotropic point sources resulting from image processing without the $F(y)$ correction factor to the measured far field along with the true diffraction limited image

that the image was distorted both in peak position and amplitude for finite apertures. Although phase correction for the constant-range and planar aperture differential distance was shown by example to be essential for imaging, useful images can be obtained by such crude approximations as making either plus or minus phase assignments to alternate lobes of the far-field pattern.

The classical Rayleigh resolution criterion was originally deduced from empirical evidence; its exact analytical basis was given in this report. The Rayleigh criterion provides a useful working rule for determining resolution capability and system requirements and expresses an arbitrary but practical limitation of resolution to the radar target imaging problem.

ACKNOWLEDGMENTS

The encouraging and enlightening discussions of various aspects of this problem with Messrs. P. J. Allen and R. D. Tompkins are gratefully acknowledged. Appreciation is also extended to Mr. C. G. Myers for consultation on special computer programming particulars.

This page intentionally left blank.

Security Classification

DOCUMENT CONTROL DATA - R & D

(Security classification of title, body of abstract and indexing annotation must be entered when the overall report is classified)

1. ORIGINATING ACTIVITY *(Corporate author)* Naval Research Laboratory Washington, D.C. 20390	2a. REPORT SECURITY CLASSIFICATION Unclassified 2b. GROUP

3. REPORT TITLE

SOME BASIC ASPECTS OF RADAR TARGET IMAGING

4. DESCRIPTIVE NOTES *(Type of report and inclusive dates)*

This is an interim report on a continuing problem.

5. AUTHOR(S) *(First name, middle initial, last name)*

Henry A. Brown

6. REPORT DATE November 15, 1967	7a. TOTAL NO. OF PAGES 28	7b. NO. OF REFS 3

8a. CONTRACT OR GRANT NO. NRL Problem R02-14 b. PROJECT NO. RF-001-02-41-4005 c. d.	9a. ORIGINATOR'S REPORT NUMBER(S) NRL Report 6623 9b. OTHER REPORT NO(S) *(Any other numbers that may be assigned this report)*

10. DISTRIBUTION STATEMENT

This document has been approved for public release and sale; its distribution is unlimited.

11. SUPPLEMENTARY NOTES	12. SPONSORING MILITARY ACTIVITY Department of the Navy (Office of Naval Research), Washington, D.C. 20360

13. ABSTRACT

The classical basis of resolution as applied to radar target imaging has been investigated with reference to point source targets in one dimension and their associated images. The imaging process can be represented by a Fourier integral operation on modified planar aperture data; two methods of evaluating this integral by a digital computer are linear interpolation and Filon's method. Curves were prepared which illustrate the aperture-resolution relationship and the sampling element placement within the aperture. Image distortion due to finite aperture size and to approximations of the far-field phase were examined by generating point source images on a computer and found to be distorted both in peak position and amplitude for finite apertures. Although phase correction for the distance between the constant-range surface and the planar aperture was shown by example to be essential for imaging, useful images can be obtained by such crude approximations as making plus or minus phase assignments to alternate lobes of the far-field pattern.

DD FORM 1 NOV 65 1473 (PAGE 1)

S/N 0101-807-6801

Security Classification

Security Classification

14. KEY WORDS	LINK A ROLE	LINK A WT	LINK B ROLE	LINK B WT	LINK C ROLE	LINK C WT
Radar target imaging						
Isotropic point source targets						
Rayleigh resolution						
Fourier integral						
Resolution						
Microwave imaging						

DD FORM 1 NOV 65 1473 (BACK) GPO 934-021

(PAGE 2)

Security Classification